Journal Name

COMMUNICATION

Visible light-initiated interfacial thiol-norbornene photopolymerization for forming islet surface conformal coating

Han Shih,[a] Raghavendra G. Mirmira,[b] and Chien-Chi Lin[a,c]

A cytocompatible visible light-mediated interfacial thiol-norbornene photopolymerization scheme was developed for creating hydrogel conformal coating on pancreatic islets. The step-growth thiol-norbornene reaction affords high consistency and tunability in gel coating thickness. Furthermore, isolated islets coated with thiol-norbornene gel maintained their viability and function *in vitro*.

Type 1 diabetes mellitus (T1DM) is an autoimmune disorder caused by auto-reactive T-cells that destroy insulin-producing pancreatic β-cells in the islets of Langerhans.[1] The destruction of β-cells leads to inadequate insulin secretion and hyperglycemia. Current standard of therapy to restore glucose homeostasis is through multiple daily insulin injections or implantation of insulin delivery devices.[2] However, tight glycemic control through insulin administration requires frequent monitoring of blood glucose levels. In addition, patients experience various degrees of discomfort from exogenous insulin delivery. While whole pancreas or islet transplantation can provide T1DM patients with insulin-independence, these approaches are reserved for diabetic patients with hypoglycemia unawareness due to a significant shortage of donor organs.[3-5] The outcome of islet transplantation, however, is heavily influenced by blood mediated inflammatory response (IBMIR), which can destroy more than half of the transplanted islets shortly after surgery.[6-8] Furthermore, patients receiving donor islets are required to undergo lifelong immunosuppressant therapy. To improve the lifespan of transplanted islets, scientists and engineers have been developing encapsulation technologies to separate allogenic or even xenogenic islets from host tissues.[9-18] A successful permselective immune isolation barrier should be able to prevent infiltration of host immune cells while permitting facile exchange of nutrients and metabolites, including oxygen, glucose, and insulin.[2]

A variety of encapsulation technologies have been developed for forming islet surface coating, including macromolecular self-assembly,[13, 15, 19] cell surface engineering,[13] and covalent cross-linking of hydrogels.[2, 20] For example, islets can be encapsulated in polyplexes formed by layer-by-layer (LbL) self-assembly of ionic macromolecules (e.g., polyanionic alginate with divalent barium or calcium cations).[21-23] Biotin-streptavidin affinity binding and hydrogen bonding between polar macromers have also been explored for forming multi-layer polymer coating for islet encapsulation.[24-26] The long-term stability of these physically assembled coatings is easily affected by tissue conditions at the transplantation site, such as pH and ionic strength.[27, 28] Alternatively, islets can be encapsulated through cell surface engineering. In one example, islets were functionalized with hetero-bifunctional maleimide-poly(ethylene glycol)-lipid (maleimide-PEG-lipid), which was conjugated with thiol-containing molecules via thiol-maleimide Michael-type addition.[29-31] Conformal coating of islets can also be formed by visible light-mediated chain-growth polymerization of acrylate-based macromers.[9, 26, 32-35] In addition to the macromer PEG-diacrylate (PEGDA), co-initiator triethanolamine (TEA) and co-monomer N-vinylpyrrolidone (NVP) are required for efficient cross-linking. This technique achieved early success in animal and non-human primate models.[36] Unfortunately, acrylate-based chain-growth polymerization is not ideal for encapsulating radical-sensitive islet cells, due in large part to the potential cytotoxicity of co-initiator (i.e., TEA),[37, 38] and the formation of a heterogeneous network containing hydrophobic polyacrylate kinetic chains.[39] It was reported that this reaction created a dense PEGDA hydrogel layer immediately adjacent to the cell surface.[32] Since the coating was formed with a gradient of cross-linking densities, the permeability of essential nutrients, oxygen, and insulin across the gel membrane may be adversely affected.[40] In this communication, we present a visible light-mediated thiol-norbornene interfacial photopolymerization for forming conformal coating on islet surface. This visible light based step-growth gelation scheme was reported previously for forming bulk or micro-scale hydrogels without using co-monomer (e.g., NVP) and amine-based co-initiator (e.g., TEA).[41-43] Mechanistically, thiol-containing molecules (e.g., DTT) serve not only as a cross-linker, but also a co-initiator. Upon visible light exposure, thiol-containing molecules are deprotonated by the excited eosin-Y, thus forming thiyl radicals that are reactive with the norbornene moieties on PEG-norbornene (PEGNB, Fig. 1a, 2a). Unlike a chain-growth network that contains heterogeneous cross-links, the step-growth thiol-norbornene photo-click reaction produces orthogonal cross-links with enhanced cytocompatibility (Fig. 2a).[41, 44, 45]

We first evaluated the cytocompatibility of cell surface initiated thiol-norbornene photo-click reaction using MIN6 β-cell aggregates as a cell model. Cell aggregates were generated from culturing cells on a rotating platform shaker. To evaluate the effect of radical-mediated photopolymerizations while excluding the influence of a cross-linked polymer network on cell viability, we used only linear macromer components that permit reactions but not gelation (Fig. 1a), PEG-mono-methacrylate (PEGMA) in chain-growth reaction and PEG-di-norbornene (PEGdNB) for step-growth reaction. After visible light exposure, significantly more dead cells were found on the surface of MIN6 cell aggregates in the chain-growth group where reaction was initiated by eosin-Y and TEA. At the same macromer reactive group concentration, chain-growth reaction was less cytocompatible compared with step-growth photo-click reaction initiated by eosin-Y and dithiothreitol (DTT).
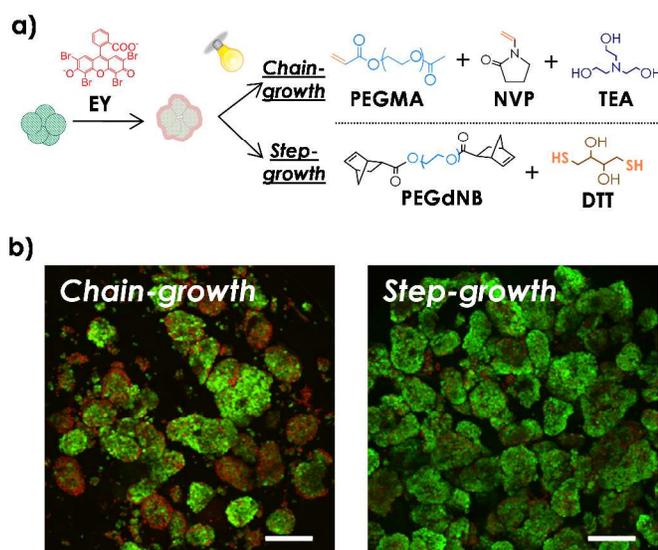

Fig. 1 (a) Schematic of visible light-mediated interfacial chain-growth (top) or step-growth thiol-norbornene (bottom) photopolymerization (EY: eosin-Y). (b) Viability of MIN6 cell aggregates after non-gelling interfacial photopolymerization reactions (Green: live cells. Red: dead cells. Scales: 100 μm).

Next, we prepared interfacial thiol-norbornene hydrogel coating on MIN6 β-cell aggregates. Eosin-Y stained cell aggregates were incubated in a precursor solution containing gelling components, including 8-arm PEG-norbornene (PEG8NB) and crosslinker DTT (Fig. S1a & 2a), and were exposed to bright visible light (30 mW/cm^2 at 555 nm). In these experiments, aggregate density was fixed at approximately 500 aggregates/mL and more than 200 aggregates were analysed. Representative phase contrast images revealed the formation of a thin thiol-norbornene hydrogel coating on the surface of cell aggregates after only 30 seconds of light exposure (Fig. 2b, left). Furthermore, live/dead staining results showed that the coated β-cell aggregates remained viable (Fig. 2c, left). However, this direct coating method (i.e., one-step incubation) produced a wider distribution of gel coating thickness, ranging from 20 μm to 60 μm (Fig. 2d), and averaged to approximately 33 μm (Fig. 2e). In addition, the one-step method only yielded a coating efficiency of 64 % (Fig. 2f), and there was a strong dependency between the coating thickness and the size of the cell aggregates (Fig. 2g). Here, coating efficiency is defined as the fraction of coated aggregates over the sum of all (coated and non-coated) aggregates. While one-step coating method is easy and cytocompatible to β-cell aggregates, it did not show high coating efficiency and consistency.

Thus, it is imperative to establish a coating strategy that provides high consistency and repeatability for isolated islets, which are heterogeneous in size (a few tens to a few hundreds micron).[46]

We hypothesized that the conformal coating results could be improved by providing additional thiols near the surface of the cell aggregates. Our recent work has shown that PEG exhibits affinity to eosin-Y.[47] Hence, we reasoned that incubating eosin-Y stained aggregates with PEG-di-thiol (PEGdSH) would allow PEGdSH to anchor on the surface of cell aggregates via affinity binding to eosin-Y that was pre-absorbed on the aggregate surface (Fig. S1b). To perform this experiment, stained aggregates were incubated in PEGdSH before suspending in macromer solution containing PEG8NB with DTT (Fig. S1b). After 30 seconds of light exposure, similar conformal hydrogel coating formed on β-cell aggregates (Fig. 2b, right). This two-step coating process was also cytocompatible to MIN6 aggregates (Fig. 2c, right). Although slightly more cell death was observed on the aggregate surface (potentially due to increased thiyl radical concentration near the surface of aggregates, Fig. 2c, right), the two-step incubation process produced thiol-norbornene conformal gel layer with a narrower distribution of coating thickness (Fig. 2d, ~20 to 40 μm) and a lower average coating thickness (Fig. 2e, 26 μm). More importantly, the two-step coating method yielded higher coating efficiency (Fig. 2f, 80 %) and a reduced dependency between coating thickness and the size of cell aggregates (Fig. 2g). Future work will focus on fine tuning the two-step coating procedure, in particular PEGdSH incubation time and concentration, to improve the viability of aggregates while maintaining the high coating efficiency.
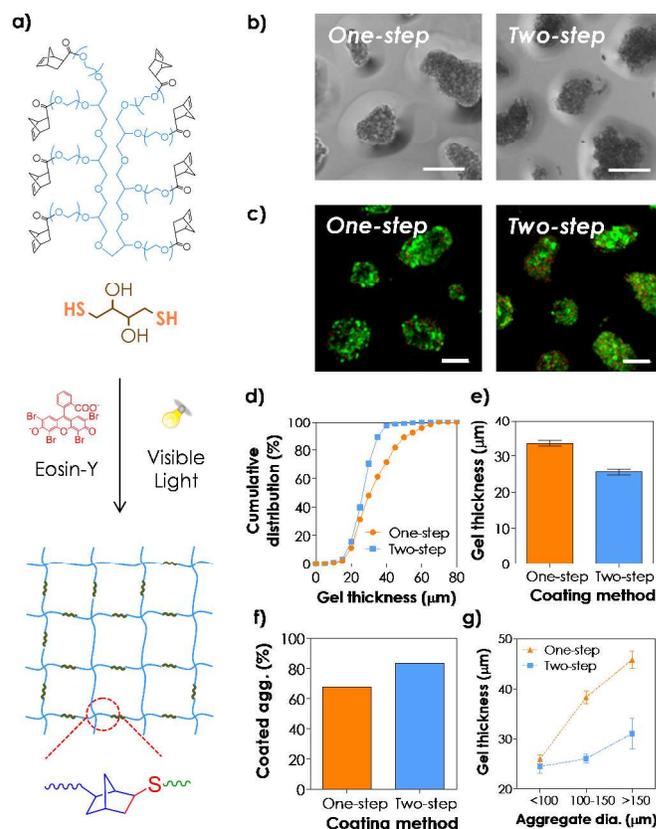

Fig. 2 (a) Schematic of visible light-mediated step-growth orthogonal thiol-norbornene reaction to form idealized hydrogel network. (b) Representative phase-contrast images of the conformal coated aggregates. (c) Representative live/dead stained images of the conformal coated aggregates (Scales: 50μm). (d-f) Effects of coating

methods on (d) the cumulative distribution of conformal gel coating thickness, (e) the average coating thickness, and (f) the percent of coated aggregates. (g) Effect of aggregate diameter on thiol-norbornene conformal coating thickness. (One-step: 20 wt% PEG8NB-DTT and 30 seconds of light exposure. Two-step: 20 wt% PEG8NB-DTT, 3.4 kDa PEGdSH and 30 seconds of light exposure. Mean ± SEM, n > 200 aggregates)

Results shown in Fig. 2 have revealed the benefits and importance of additional PEGdSH incubation in interfacial thiol-norbornene photopolymerization. Therefore, we further investigated the effect of PEGdSH on coating thickness and efficiency. In general, the thiol-norbornene coating thickness decreased with increasing molecular weight (MW) of PEGdSH (i.e., from 35 µm, 26 µm, to 13 µm for 2 kDa, 3.4 kDa, and 10 kDa PEGdSH, respectively, Fig. 3a-d & S2a). The use of higher MW of PEGdSH resulted in decreased coating efficiency (Fig. S2b, from 98 % to 64 %). It is worth mentioning that in these experiments, the concentration of PEGdSH was maintained at 20 wt%. PEGdSH at a lower MW has higher thiol content when comparing with its counterpart at a higher MW and at the same macromer concentration. Therefore, increased coating thickness and efficiency at a lower PEGdSH MW were likely a result of increased availability of thiols near the surface of the aggregates, which accelerated the thiol-norbornene cross-linking reaction.
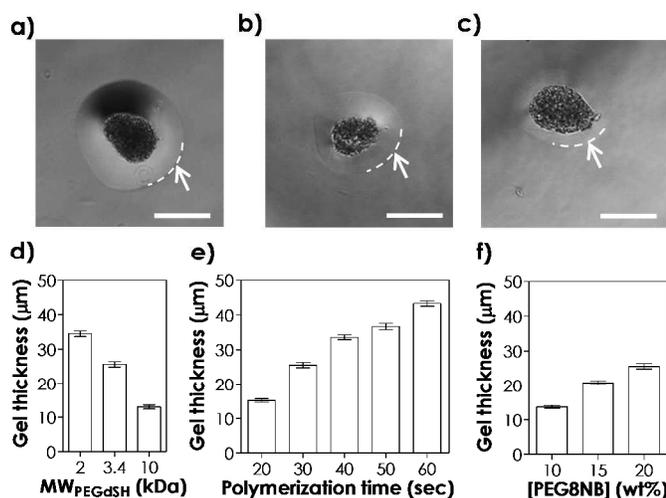

Fig. 3 (a-c) Representative phase-contrast images of MIN6 cell aggregates with thiol-norbornene conformal gel coating (two-step coating method). PEGdSH MW: (a) 2 kDa, (b) 3.4 kDa, and (c) 10 kDa. Arrows and dashed lines indicate the boundary of the hydrogel coating (Scales: 50 µm). (d-f) Parameters affecting thiol-norbornene conformal coating thickness: (d) molecular weight of PEGdSH, (e) photopolymerization time, and (f) concentration of macromer PEG8NB. Coating conditions: (a-d) 20 wt% of PEG8NB-DTT and 30 seconds of light exposure. (e) 20 wt% of PEG8NB-DTT and 3.4 kDa of PEGdSH. (f) 3.4 kDa of PEGdSH and 30 seconds of light exposure (Mean ± SEM, n > 200 aggregates).

When the polymerization time was increased from 20 to 60 seconds, gel thickness also increased (from 15 to 43 µm, Fig. 3e & S3a). Longer polymerization time resulted in higher coating efficiency (from 53 % to 98 %, Fig. S3b) but also increased the likelihood of encapsulating more than one aggregate per gel capsule (~20 % at 60 seconds). The later would increase the volume of the islet transplants and might not be ideal for minimally invasive surgery. A large graft volume also increases diffusion path, which

could reduce the responsiveness of the encapsulated islets to glucose. When the concentration of PEG8NB in the precursor solution was increased from 10 wt% to 20 wt%, gel thickness increased from 14 to 26 µm (Fig. 3f & S4a). The use of a higher PEG8NB concentration also increased coating efficiency (from 24 % to 84 %, Fig. S4b). Using bulk thiol-norbornene hydrogels, we showed that the mesh size of these step-growth hydrogels depends on the concentration of PEG8NB. Based on the known average molecular weight between crosslinks and the Flory-Rehner theory of elasticity, the mesh size of a step-growth hydrogel with an ideal network (e.g., PEG8NB-DTT hydrogel) should be 9.1 nm (Equation S1 to S6).[48] The mesh sizes of all thiol-norbornene hydrogels prepared here (Fig. S5a, from 15.1 nm to 9.9 nm for 5 to 20 wt% of PEG8NB, respectively) were all much larger than the hydrodynamic radius of insulin (Fig. S5a, $R_{H,ins}$ = 2.0 nm).[49] Furthermore, we estimated that the diffusion coefficients of insulin (D_g) are between 1260 to 980 $µm^2$/sec (Fig. S5b) in thiol-norbornene hydrogels prepared from 5 to 20 wt% of PEG8NB. The diffusivities of insulin in the swollen hydrogel were slightly lower than that in aqueous buffer solution (D_0: ~1500 $µm^2$/sec).[50] These estimations suggest that the diffusion of insulin from the highly swollen thiol-norbornene hydrogels will be affected only minimally.

Following the optimization of interfacial thiol-norbornene photopolymerization conditions using MIN6 cell aggregates, we prepared orthogonal thiol-norbornene hydrogel conformal coating on isolated mouse islets. Here, a non-degradable macromer PEGaNB was used to coat islets for long-term culture. It is worth mentioning that thiol-norbornene hydrogels formed from PEGa8NB have similar degree of cross-linking efficiency (i.e., gel fraction above 90 %) and swelling (up to 2 weeks) when compared with hydrolytically labile ester-containing PEG8NB (Fig. S6). While hydrogels formed from hydrolytically labile PEG8NB showed significant degradation after three weeks in PBS, no gel degradation was observed in gels formed from hydrolytically stable PEGa8NB (Fig. S6c). As shown in Fig. 4a, islets coated via visible light-mediated interfacial thiol-norbornene photopolymerization remained viable. Furthermore, the hydrogel layer maintained its stability throughout 2 weeks of *in vitro* culture (Fig. 4b, 4c & 4d). The average thickness of the conformal coating was about 37 µm with 90 % of coating efficiency (data not shown). In long-term *in vitro* culture of primary islets (14 days), we observed the darkening of islets core. This phenomenon was common in islet culture as previously reported by Dionne *et al.* The authors attributed the result to necrosis at the islet core.[51] As can be seen in Fig. 4c (top), the cellular debris was found free floating in culture media with the non-coated islets. On the other hand, the dark debris was 'trapped' within the conformal coating layer on the coated islets. These results suggest that the coating could serve as a bi-directional barrier for blocking the infiltration of host immune cells, and for preventing the liberation of graft debris to the transplantation site that would otherwise trigger host immune response.[52, 53] Future work will focus on addressing the inflammatory response of coated islets *in vivo* using mouse models.

To examine insulin secretion from the coated islets, static glucose-stimulated insulin secretion (GSIS) was performed at day 2 and day 14 (Fig. 4e & 4f). Within each non-coated or coated islets group, statistically significance (p < 0.05) was found between insulin secretion at 2.5 mM and 25 mM glucose. Based on the results of GSIS index, which is the ratio of insulin secretion in high glucose buffer to low glucose buffer, we found no statistical significance between thiol-norbornene hydrogel coated and non-coated islets throughout 2 weeks of *in vitro* culture (Fig. S7). The results of static GSIS test suggest that the islets remained viable and functional after thiol-norbornene conformal gel coating. In Fig. 4d and 4e, the amounts of insulin secretion by the coated islets are significantly

higher than the non-coated islets (Fig. 4d and 4e). This might be the stress induced by gel coating on the surface of islets (Fig. 4a, bottom). While static GSIS results here have revealed that the thiol-norbornene gel coated islets remained viable and functional, future experiments will include glucose perfusion GSIS study to ensure that the hydrogel coating does not negatively affect insulin release dynamics.
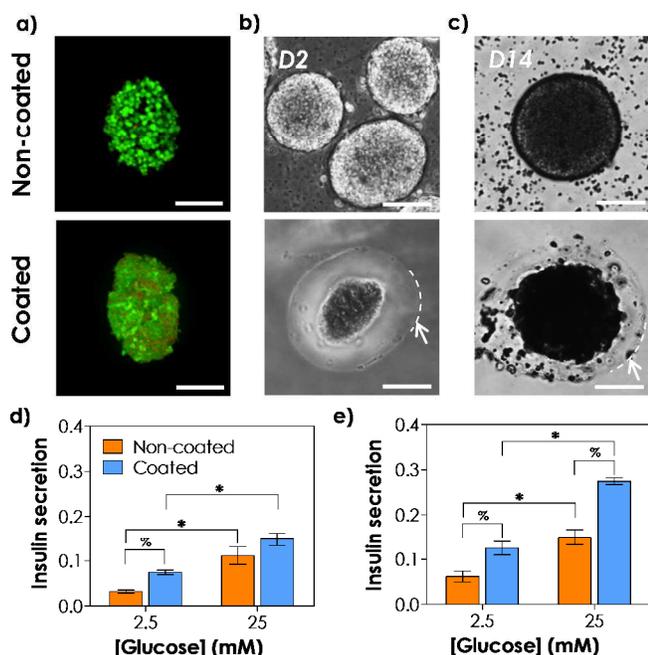

Fig. 4 (a) Representative live/dead stained images of non-coated and coated CD1 mice islets (24 hours after coating). (b-c) Representative phase contrast images of non-coated (top) and coated (bottom) CD1 mice islets on day 2 (b), and day 14 (c). Arrows and dashed lines in (b-c) indicate the boundary of the hydrogel coating (Scales: 50 μm). (d-e) *In vitro* glucose stimulated insulin secretion (GSIS) of isolated islets on (d) day 2 and (e) day 14. Asterisks (*) and percent signs (%) indicate statistical significance between 2.5 and 25 mM of glucose within each group, and between non-coated and coated islets within each glucose concentration (Mean ± SEM, $p < 0.05$), respectively. Coating conditions: 3.4 kDa PEGdSH, 20 wt% PEGa8NB-DTT, 25 seconds light exposure.

Conclusions

In summary, we have developed a visible light-mediated thiol-norbornene interfacial coating process to prepare step-growth conformal hydrogel coating on islet surface. Using MIN6 β-cell aggregates as a model, we evaluated the parameters critical in determining coating thickness (e.g., MW of PEGdSH, polymerization time, and macromer concentration). The results of live/dead staining and GSIS demonstrated high cytocompatibility of thiol-norbornene hydrogel coating on murine islets. This visible light mediated thiol-norbornene interfacial photopolymerization provides an alternate coating option and should be of great interest to the field of islet transplantation. Future work will focus on modifying thiol-norbornene gel formulation to create multi-functional immuno-isolation barrier, and on determining the inflammatory response and long-term efficacy of the transplanted coated islets on maintaining euglycemia.

Notes

[a] Weldon School of Biomedical Engineering, Purdue University, West Lafayette, IN, USA.
[b] Departments of Pediatrics, Medicine, Cellular and Integrative Physiology, and Biochemistry and Molecular Biology, Indiana University School of Medicine, Indianapolis, IN, USA.
[c] Department of Biomedical Engineering, Indiana University-Purdue University Indianapolis, Indianapolis, IN, USA
† Electronic Supplementary Information (ESI) available: materials and method and additional data.

References

1. R. P. Robertson, C. Davis, J. Larsen, R. Stratta and D. E. Sutherland, *Diabetes care*, 2000, **23**, 112-116.
2. K. M. Bratlie, R. L. York, M. A. Invernale, R. Langer and D. G. Anderson, *Advanced healthcare materials*, 2012, **1**, 267-284.
3. A. M. Shapiro, J. R. Lakey, E. A. Ryan, G. S. Korbutt, E. Toth, G. L. Warnock, N. M. Kneteman and R. V. Rajotte, *The New England journal of medicine*, 2000, **343**, 230-238.
4. E. A. Ryan, J. R. Lakey, R. V. Rajotte, G. S. Korbutt, T. Kin, S. Imes, A. Rabinovitch, J. F. Elliott, D. Bigam, N. M. Kneteman, G. L. Warnock, I. Larsen and A. M. Shapiro, *Diabetes*, 2001, **50**, 710-719.
5. P. Soon-Shiong, R. E. Heintz, N. Merideth, Q. X. Yao, Z. Yao, T. Zheng, M. Murphy, M. K. Moloney, M. Schmehl, M. Harris and et al., *Lancet*, 1994, **343**, 950-951.
6. B. Nilsson, K. N. Ekdahl and O. Korsgren, *Current opinion in organ transplantation*, 2011, **16**, 620-626.
7. L. Moberg, H. Johansson, A. Lukinius, C. Berne, A. Foss, R. Kallen, O. Ostraat, K. Salmela, A. Tibell, G. Tufveson, G. Elgue, K. Nilsson Ekdahl, O. Korsgren and B. Nilsson, *Lancet*, 2002, **360**, 2039-2045.
8. A. M. Shapiro, C. Ricordi, B. J. Hering, H. Auchincloss, R. Lindblad, R. P. Robertson, A. Secchi, M. D. Brendel, T. Berney, D. C. Brennan, E. Cagliero, R. Alejandro, E. A. Ryan, B. DiMercurio, P. Morel, K. S. Polonsky, J. A. Reems, R. G. Bretzel, F. Bertuzzi, T. Froud, R. Kandaswamy, D. E. Sutherland, G. Eisenbarth, M. Segal, J. Preiksaitis, G. S. Korbutt, F. B. Barton, L. Viviano, V. Seyfert-Margolis, J. Bluestone and J. R. Lakey, *The New England journal of medicine*, 2006, **355**, 1318-1330.
9. A. S. Sawhney and J. A. Hubbell, *Biomaterials*, 1992, **13**, 863-870.
10. T. Wang, I. Lacik, M. Brissova, A. V. Anilkumar, A. Prokop, D. Hunkeler, R. Green, K. Shahrokhi and A. C. Powers, *Nature biotechnology*, 1997, **15**, 358-362.
11. T. M. Chang, *Nature reviews. Drug discovery*, 2005, **4**, 221-235.
12. M. Y. Fan, Z. P. Lum, X. W. Fu, L. Levesque, I. T. Tai and A. M. Sun, *Diabetes*, 1990, **39**, 519-522.
13. Y. Teramura and H. Iwata, *Advanced drug delivery reviews*, 2010, **62**, 827-840.
14. D. B. Jaroch, J. Lu, R. Madangopal, N. D. Stull, M. Stensberg, J. Shi, J. L. Kahn, R. Herrera-Perez, M. Zeitchek, J. Sturgis, J. P. Robinson, M. C. Yoder, D. M. Porterfield, R. G. Mirmira and J. L. Rickus, *American journal of physiology. Endocrinology and metabolism*, 2013, **305**, E1230-1240.
15. E. S. O'Sullivan, A. Vegas, D. G. Anderson and G. C. Weir, *Endocrine reviews*, 2011, **32**, 827-844.
16. M. Ma, A. Chiu, G. Sahay, J. C. Doloff, N. Dholakia, R. Thakrar, J. Cohen, A. Vegas, D. Chen, K. M. Bratlie, T. Dang, R. L. York, J. Hollister-Lock, G. C. Weir and D. G. Anderson, *Advanced healthcare materials*, 2013, **2**, 667-672.

17. H. R. Rengifo, J. A. Giraldo, I. Labrada and C. L. Stabler, *Advanced healthcare materials*, 2014.
18. K. M. Gattás-Asfura and C. L. Stabler, *ACS Applied Materials & Interfaces*, 2013, **5**, 9964-9974.
19. S. Kizilel, M. Garfinkel and E. Opara, *Diabetes technology & therapeutics*, 2005, **7**, 968-985.
20. J. T. Wilson and E. L. Chaikof, *Advanced drug delivery reviews*, 2008, **60**, 124-145.
21. B. Thu, P. Bruheim, T. Espevik, O. Smidsrod, P. Soon-Shiong and G. Skjak-Braek, *Biomaterials*, 1996, **17**, 1031-1040.
22. F. Lim and A. M. Sun, *Science*, 1980, **210**, 908-910.
23. P. de Vos, M. M. Faas, B. Strand and R. Calafiore, *Biomaterials*, 2006, **27**, 5603-5617.
24. S. Kizilel, A. Scavone, X. Liu, J. M. Nothias, D. Ostrega, P. Witkowski and M. Millis, *Tissue engineering. Part A*, 2010, **16**, 2217-2228.
25. N. Marek, A. Krzystyniak, I. Ergenc, O. Cochet, R. Misawa, L. J. Wang, K. Golab, X. Wang, G. Kilimnik, M. Hara, S. Kizilel, P. Trzonkowski, J. M. Millis and P. Witkowski, *Annals of surgery*, 2011, **254**, 512-518; discussion 518-519.
26. G. M. Cruise, D. S. Scharp and J. A. Hubbell, *Biomaterials*, 1998, **19**, 1287-1294.
27. V. Kozlovskaya, E. Kharlampieva, I. Drachuk, D. Cheng and V. V. Tsukruk, *Soft Matter*, 2010, **6**, 3596-3608.
28. B. S. Kim, H. I. Lee, Y. Min, Z. Poon and P. T. Hammond, *Chemical communications*, 2009, 4194-4196.
29. Y. Teramura, O. P. Oommen, J. Olerud, J. Hilborn and B. Nilsson, *Biomaterials*, 2013, **34**, 2683-2693.
30. N. M. Luan and H. Iwata, *Biomaterials*, 2013, **34**, 5019-5024.
31. N. M. Luan, Y. Teramura and H. Iwata, *Biomaterials*, 2011, **32**, 6487-6492.
32. G. M. Cruise, O. D. Hegre, D. S. Scharp and J. A. Hubbell, *Biotechnology and bioengineering*, 1998, **57**, 655-665.
33. G. M. Cruise, O. D. Hegre, F. V. Lamberti, S. R. Hager, R. Hill, D. S. Scharp and J. A. Hubbell, *Cell transplantation*, 1999, **8**, 293-306.
34. A. S. Sawhney, C. P. Pathak and J. A. Hubbell, *Biomaterials*, 1993, **14**, 1008-1016.
35. A. S. Sawhney, C. P. Pathak and J. A. Hubbell, *Biotechnology and bioengineering*, 1994, **44**, 383-386.
36. C. Halberstadt and D. Emerich, in *Cellular Transplantation From Laboratory to Clinic*, Academic Press, 2006.
37. A. Shikanov, R. M. Smith, M. Xu, T. K. Woodruff and L. D. Shea, *Biomaterials*, 2011, **32**, 2524-2531.
38. E. A. Phelps, N. O. Enemchukwu, V. F. Fiore, J. C. Sy, N. Murthy, T. A. Sulchek, T. H. Barker and A. J. García, *Advanced Materials*, 2012, **24**, 64-70.
39. S. Lin-Gibson, R. L. Jones, N. R. Washburn and F. Horkay, *Macromolecules*, 2005, **38**, 2897-2902.
40. T. Bal, B. Kepsutlu and S. Kizilel, *Journal of Biomedical Materials Research Part A*, 2014, **102**, 487-495.
41. H. Shih and C. C. Lin, *Macromol Rapid Commun*, 2013, **34**, 269-273.
42. A. K. Fraser, C. S. Ki and C.-C. Lin, *Macromolecular Chemistry and Physics*, 2014, **215**, 507-515.
43. H. Shih, A. K. Fraser and C. C. Lin, *ACS Appl Mater Interfaces*, 2013, **5**, 1673-1680.
44. C. C. Lin, A. Raza and H. Shih, *Biomaterials*, 2011, **32**, 9685-9695.
45. J. D. McCall and K. S. Anseth, *Biomacromolecules*, 2012, **13**, 2410-2417.
46. M. A. von Mach, J. Schlosser, M. Weiland, P. J. Feilen, M. Ringel, J. G. Hengstler, L. S. Weilemann, J. Beyer, P. Kann and S. Schneider, *Acta diabetologica*, 2003, **40**, 123-129.
47. H. Shih, A. K. Fraser and C.-C. Lin, *ACS Applied Materials & Interfaces*, 2013, **5**, 1673-1680.
48. P. J. Flory, *Principles of Polymer Chemistry*, Cornell University Press, Ithaca, NY, 1953.
49. V. Banerjee, R. K. Kar, A. Datta, K. Parthasarathi, S. Chatterjee, K. P. Das and A. Bhunia, *PLoS ONE*, 2013, **8**, e72318.
50. P. Buchwald and S. R. Cechin, *Journal of Biomedical Science and Engineering*, 2013, **6**.
51. K. E. Dionne, C. K. Colton and M. L. Yarmush, *Diabetes*, 1993, **42**, 12-21.
52. T. Kobayashi, G. Harb, R. V. Rajotte, G. S. Korbutt, A. G. Mallett, H. Arefanian, D. Mok and G. R. Rayat, *Xenotransplantation*, 2006, **13**, 547-559.
53. V. Vaithilingam, C. Fung, S. Ratnapala, J. Foster, V. Vaghjiani, U. Manuelpillai and B. E. Tuch, *PLoS ONE*, 2013, **8**, e59120.

Journal of Materials Chemistry B Accepted Manuscript

TOC